Tunable Magnetic Properties of (Gd,Ce) 2 O 2 S Oxysulfide Nanoparticles

Clément Larquet, Yannick Klein, David Hrabovsky, Andrea Gauzzi, Clément Sanchez, Sophie Carenco

Tunable Magnetic Properties of $(Gd,Ce)_2O_2S$ Oxysulfide Nanoparticles

*Clément Larquet,[1,2] Yannick Klein,[2] David Hrabovsky,[2] Andrea Gauzzi,[2] Clément Sanchez,[1] Sophie Carenco[1,]**

[1] Sorbonne Université, CNRS UMR 7574, Collège de France, Laboratoire de Chimie de la Matière Condensée de Paris (LCMCP), 4 place Jussieu, 75252 Paris Cedex 05, France

[2] Institut de Minéralogie de Physique des Matériaux et de Cosmochimie (IMPMC), Sorbonne Université, CNRS UMR 7590, IRD UMR 206, MNHN, 4 place Jussieu 75252 Paris Cedex 05, France

* Corresponding author e-mail: sophie.carenco@sorbonne-universite.fr

Abstract:

Nanoparticles with strong paramagnetic responses are of prime interest for advanced MRI imaging. To replace Gd expensive and toxic complexes, Gd-based nanoparticles have emerged as a viable solution for efficient and harmless MRI contrast agents. Gadolinium oxysulfide nanoparticles could represent suitable candidates for MRI imaging and bimodal imaging thanks to their excellent properties as host matrix and chemical stability, but their magnetic properties at the nanoscale have been hitherto poorly investigated especially in the case of ultrafine nanoparticles (< 10 nm), where surface effects and ligands can significantly affect the magnetic behavior. In the present work, we synthesized and characterized bimetallic $(Gd,Ce)_2O_2S$ nanoparticles and demonstrated that they are paramagnetic over a wide

temperature range including the body one. The mixture of Gd and Ce magnetic centers enables a fine control of the magnetic properties up to high Ce concentrations (80 %) and over a large range of magnetic moments, while photoemission properties are guaranteed up to 20 % of Ce owing to a regular dispersion of the Ce centers. The present study on bimetallic oxysulfide nanoparticles with high concentrations of two lanthanides shows that $(Gd,Ce)_2O_2S$ nanoparticles are viable candidates as tunable nanoscaled agents for bimodal imaging.

Keywords: gadolinium oxysulfide, nanoparticles, lanthanides, tunable magnetic moment.

1. Introduction

Lanthanides can exhibit high magnetic susceptibility, which is of major interest for chemicals to be injected in a living organism. For instance, Gd^{III} complexes are used as positive contrast agents in magnetic resonance imaging (MRI) due to the $4f^7$ electronic configuration of the ion (μ_{eff} = 7.94 μ_B). Gadolinium ions in molecular complexes remain toxic because of polarizing effects and competition with calcium. Special hydrosoluble complexes were then developed to mitigate the toxicity of Gd^{III}.[1]

An alternative to lanthanide complexes is offered by lanthanide nanoparticles which display better relaxations because, in these particles, several thousand atoms are concentrated in a little volume. Iron oxide nanoparticles have also been used as negative contrast agents, however they often produce artefacts in the MRI images.[2] Gd_2O_3 nanoparticles were found to have similar or better relaxation properties than Gd complexes, without the drawbacks of iron oxides. These particles were then chosen for the precise visualization of locally injected cells.[3,4]

Doped gadolinium oxide nanoparticles were then employed for bimodal imaging (MRI and luminescence).[5] Because of their very good luminescence properties, similar results are expected for oxysulfide Gd_2O_2S nanoparticles. Bimodal agents are especially useful to probe the chemical environment of the nanoparticles by analyzing the changes of luminescence properties (wavelength, lifetime, etc.). These properties can be measured during short times and their analysis can be coupled with data obtained for long times and precise localization by means of magnetic resonance imaging.[6]

In future applications, improving the size and morphology control of Gd_2O_2S nanoparticles will be a key to make them compatible with biomedical applications, for reproducibility and regulation purposes. Prior to this, a better understanding of their intrinsic properties has to be reached. Indeed, although the literature on Ln_2O_2S nanoparticles synthesis is now well documented,[7–14] only a few reports on the properties of lanthanide oxysulfide nanoparticles are available. In 2012, He *et al.* synthesized and characterized the $Eu_{2+x}O_2S$ nanorods obtained using a single source precursor prepared *in situ* by hot injection of diethylammonium diethyldithiocarbamate (dea-ddtc) at 320 °C in a mixture of europium oleate, oleylamine and 1,10-phenanthroline and dodecanethiol.[15] Non-stoichiometry is attributed to the presence of Eu^{II} in the solid and was already observed for the bulk phase in the 1960's by Ballestracci and Quezel who estimated that 1 % of the Eu atoms are divalent from neutron diffraction and magnetic measurements.[16,17] He *et al.* also described magnetic properties of europium oxysulfide nanoparticles and confirmed the Eu^{II}:Eu^{III} ratio, even if the estimated average composition $Eu_{2.11}O_2S$ would correspond to about 15 % of Eu^{II}. In 2013, Ajithkumar *et al.* confirmed the potential use of Gd_2O_2S:Yb,Er magnetic and upconverting phosphors for bimodal imaging. Both MRI imaging and infrared imaging could be performed with the same set of nanoparticles, and the nanomaterials were shown to be non toxic.

Recently, we succeeded in synthesizing crystalline $Gd_{2(1-y)}Ce_{2y}O_2S$ bimetallic oxysulfide nanoparticles (Figure S1). Although Ce_2O_2S nanoparticles are sensitive to air and water and degrade completely within a few days, the bimetallic nanoparticles remain stable in air during several months even if they contain high amounts of cerium (up to y = 80 %). The synthesis in organic medium at relatively low temperature (310 °C) enabled the formation of a Gd_2O_2S - Ce_2O_2S solid solution, whereas classical solid-state syntheses would lead to a mixture of the two compounds. To the best of our knowledge, bimetallic oxysulfides containing high proportion of the two ions have not been previously studied, which motivates the present systematic study of their magnetic properties. Specifically, we report on the paramagnetic behavior of $Gd_{2(1-y)}Ce_{2y}O_2S$ bimetallic oxysulfide nanoparticles down to 5 K. We are interested in the tunable magnetic moment, which is due to the different number of lone electrons of gadolinium ($4f^7$) and cerium ($4f^1$). The present study also raises the question of the size effect on the magnetic properties of the Gd_2O_2S nanoparticles.

2. Results and discussion

Bulk lanthanide oxysulfides Ln_2O_2S (Ln = lanthanide) are paramagnetic compounds at ambient temperature. At low temperatures, the compounds with Ln = Gd, Tb, Dy, Ho and Yb order antiferromagnetically at Néel temperatures between 2.5 K (for Ho) and 7.7 K (for Tb) and exhibit Weiss constants, θ, between - 8 K (for Ho) and - 18 K (for Gd). The other compounds, including Ce_2O_2S, remain paramagnetic down to 2 K.[17] Gd_2O_2S is also paramagnetic in a wide range of temperature but orders antiferromagnetically at very low temperature.[16] Ballestracci *et al.* studied the Ln_2O_2S bulk compounds by neutron diffraction and estimated the Néel temperature (T_N) of Gd_2O_2S to be 5.7 K. In the paramagnetic phase, its Curie-Weiss temperature (T_{CW}) is - 18 K. The magnetic moment of Gd atoms (7.92 μ_B) was very close to these of the isolated paramagnetic ion (7.94 μ_B). In 2014, Biondo *et al.* revisited

the properties of Ln_2O_2S oxysulfides (Ln = Sm, Eu, Gd).[18] In the case of Gd_2O_2S, the reported properties are close to those of Ballestracci *et al.*, i.e. T_N = 5.8 K, T_C = - 21.3 K. This indicates the existence of a geometric magnetic frustration due to the triangular lattice.[19]

In the $Gd_{2(1-y)}Ce_{2y}O_2S$ nanoparticles, Ce^{III} luminescence could be detected and measured between 420 and 650 nm for the samples with y = 2 % and 20 % (Figure S4). This shows the relevance of these objects for further luminescence application in the visible range.

In view of the above results, we expect similar paramagnetic properties in $Gd_{2(1-y)}Ce_{2y}O_2S$ nanoparticles, which display a tunable concentration of cerium (Figure S2) and keep the Ln_2O_2S structure up to y = 80 % (Figure S3). Specifically, the paramagnetic response of the powders should decrease with y. Nevertheless, the coupling between gadolinium and cerium ions is possible because both ions have partially occupied *f* orbitals. Zero-field cooling (ZFC) curves were measured by vibrating sample magnetometry (VSM) on the powders and plotted in Figure 1. A conventional paramagnetic response was observed in the whole 5 – 350 K range. The field-cooling (FC) curves were identical to the ZFC ones.

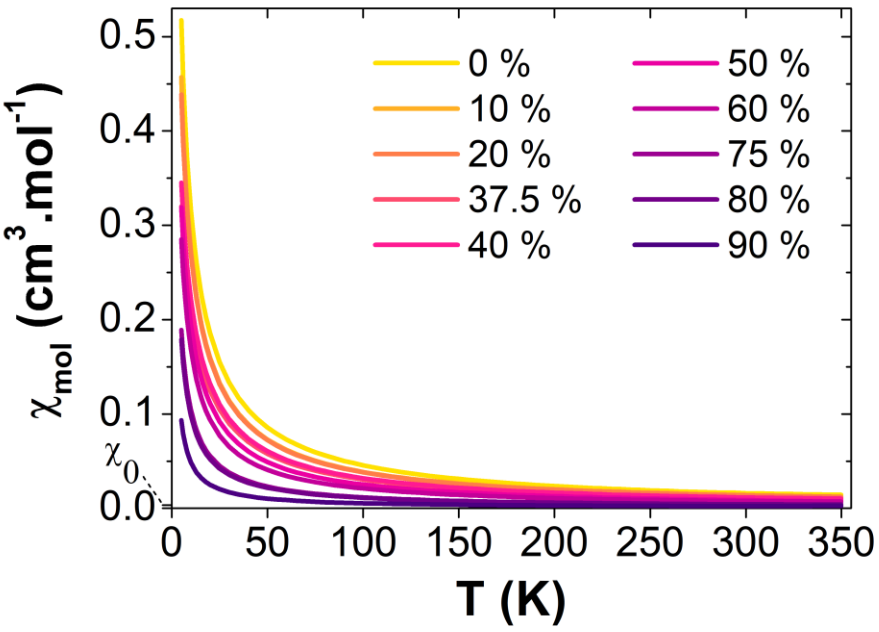

Figure 1: Molar susceptibility χ_{mol} of $Gd_{2(1-y)}Ce_{2y}O_2S$ powders measured by vibrating sample magnetometry. The average value of χ_0 is indicated on the ordinate axis. The y value is indicated in % in the legend. The applied field is 50 Oe.

We were able to fit the $\chi_{mol}(T)$ curves using a generalized Curie's law, as demonstrated in Figure 2. The constant contribution χ_0 is orders of magnitude smaller than the total susceptibility at low temperature (for $y = 0 – 80$ %: at 5 K, $\chi_{mol} > 150\,\chi_0$; at 100 K, $\chi_{mol} > 10\,\chi_0$). In a paramagnetic system, this term typically describes core diamagnetism or Pauli paramagnetism. In the present case, χ_0 takes into account the contribution of the sample holder and of the organic ligands on the surface of the nanoparticles. For all compositions, the value of θ falls in the 0 – 2 K range, thus indicating negligible magnetic fluctuations.

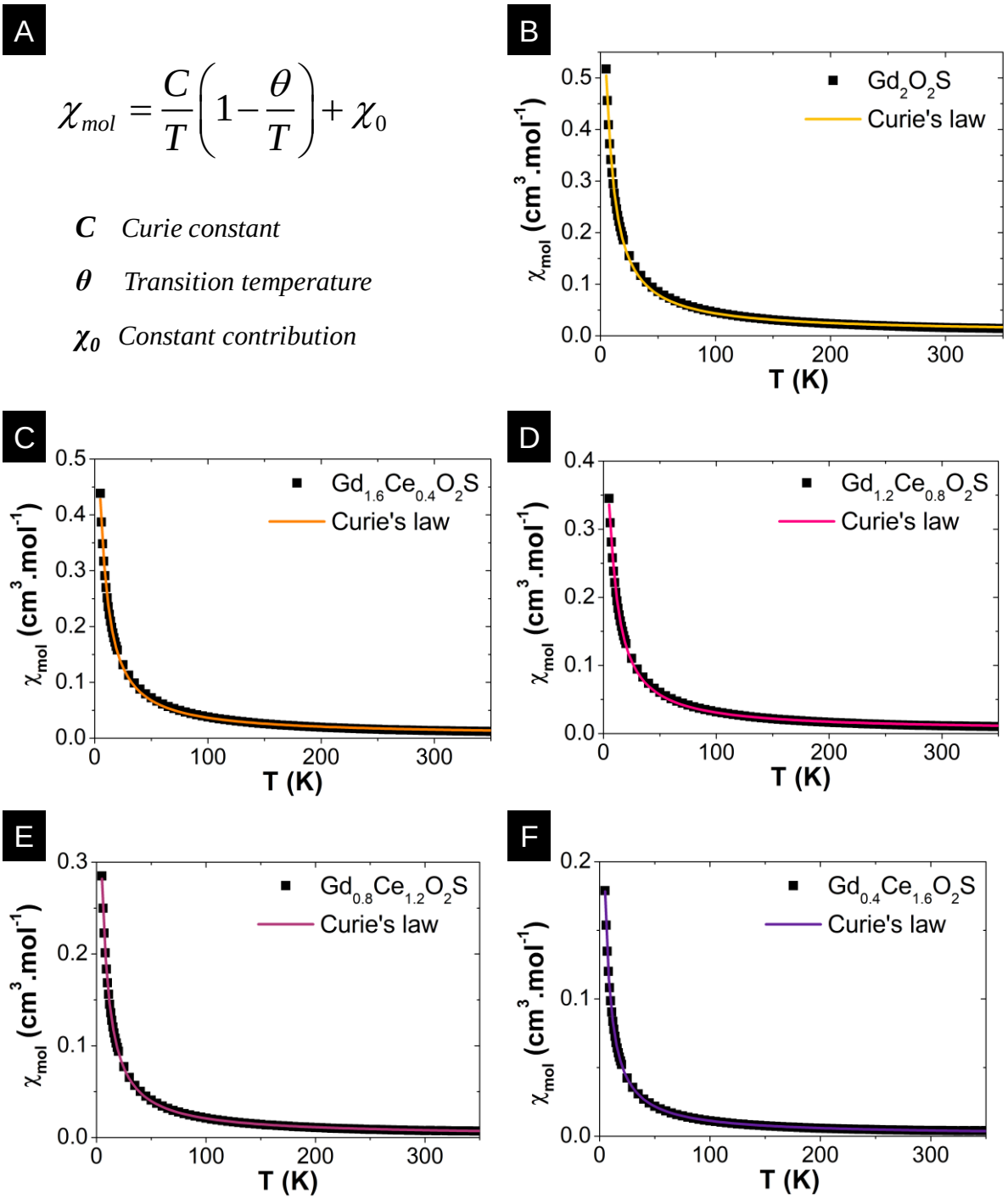

Figure 2: (A) Generalized Curie law. Fit of the ZFC molar susceptibility $\chi_{mol}(T)$ of the Gd_2O_2S (B), $Gd_{1.6}Ce_{0.4}O_2S$ (C), $Gd_{1.2}Ce_{0.8}O_2S$ (D), $Gd_{0.8}Ce_{1.2}O_2S$ (E) and $Gd_{0.4}Ce_{1.6}O_2S$ (F) nanoparticle samples by using the generalized Curie's law.

The expression of the Curie constant, *C*, as defined in Figure 2A is given in Equation 1.

$$C = \frac{N\mu_B^2}{3k_B} g^2 J(J+1)$$

$\boldsymbol{N}$	*Avogadro constant*
$\boldsymbol{\mu_B}$	*Bohr magnetron*
$\boldsymbol{k_B}$	*Boltzmann constant*
$\boldsymbol{g}$	*Landé factor*
$\boldsymbol{J}$	*Angular momentum quantum number*

Equation 1: Expression of the Curie constant.

Equation 2 describes the relation between the effective magnetic moment, the Landé factor and the angular momentum quantum number.

$$\mu_{eff} = g\sqrt{J(J+1)}$$

Equation 2: Expression of the effective magnetic moment.

From Equation 1 and Equation 2, the magnetic moment is proportional to the square root of the Curie constant's, as indicated in Equation 3.

$$\mu_{eff}^2 = \frac{3k_B C}{N\mu_B^2} \simeq 8.00C$$

Equation 3: Approximated expression of the square effective magnetic moment, obtained with N = 6.02 x 10^{23} mol^{-1}, k_B = 1.38 x 10^{-16} erg/K and μ_B = 9.27 x 10^{-21} erg/G.

The values of the susceptibility and of the magnetic moments were corrected to take into account the oleate organic ligands (30 % of the sample in mass). Within a simple model of paramagnetic impurities, the above analysis explains well the linear dependence of the square

of the magnetic moment on composition (Figure 3). The linear dependence of $(\mu_{eff})^2$ *vs.* *y* is therefore consistent with a picture of solid solution of gadolinium and cerium atoms in the nanoparticles. This linear dependence is observed up to *y* = 60 %.

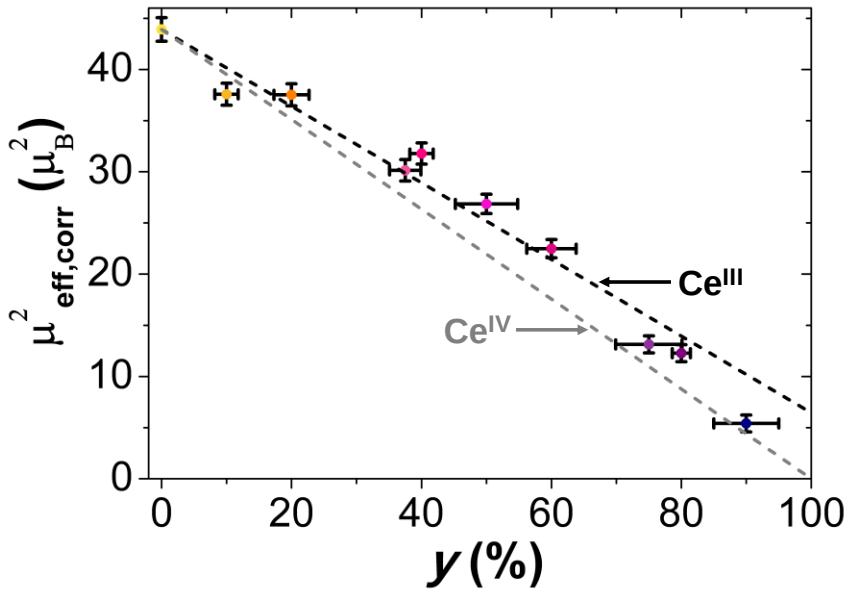

Figure 3: Experimental dependence of the square magnetic moments of $Gd_{2(1-y)}Ce_{2y}O_2S$ nanoparticles on *y*. The raw values of magnetic susceptibility have been normalized by assuming that 30 wt% of the samples is made of oleate ligands. The broken black and gray lines indicate the dependence expected in the case of Ce^{III} or Ce^{IV} cations, respectively.

For concentrations above 60 %, a downward deviation from the linear dependence was observed. We attribute this to the partial oxidation of Ce^{III} into Ce^{IV}, as discussed by some of us in a previous work.[14] This deviation is even more parked for *y* > 80 %, in the range of composition where a degradation of the nanoparticles occurs. Because the *y* = 100 % sample (Ce_2O_2S nanoparticles) is highly sensitive in air, no magnetic measurement was carried out.

Conclusion

In the present work, we have carried out a systematic study of the magnetic properties of $Gd_{2(1-y)}Ce_{2y}O_2S$ in a wide range of composition, y = 0 - 90 %. We have found that the nanoparticles are paramagnetic in the whole 5 – 350 K temperature range studied and the temperature dependence of the susceptibility is well described by a generalized Curie law. Our data analysis indicates that the magnetic moment linearly decreases with Ce concentration, as expected from a simple ionic model suitable to describe the electronic configuration of the *4f* shell. The above results indicate that the magnetic properties of the $Gd_{2(1-y)}Ce_{2y}O_2S$ nanoparticles are easily tuned by chemical composition in a wide range, y = 0 - 80 %. For y > 60 %, Ce oxidation is significant and leads to a decrease of the expected magnetic moment. Remarkably, the Gd_2O_2S nanocrystals do not exhibit antiferromagnetic order down to 5 K, contrary to the bulk, which displays an order at 5.7 K. The reason for this difference, which we tentatively attribute to size effects, will be the object of a future work.

Altogether, the combination of tunable paramagnetic and photoluminescence properties is promising for the development of $Gd_{2(1-y)}Ce_{2y}O_2S$ nanoparticles for bimodal imaging applications. Indeed, Ce^{III} cations emit light even for relatively high doping concentrations. Future directions of work include the study of size-effect on the magnetic properties, which should be performed on nanoplates with a narrower width distribution. They also encompass the evaluation of *in vitro* and *in vivo* toxicity of the nanoparticles, which will be reported in due time.

Experimental section

Synthesis of $Gd_{2(1-y)}Ce_{2y}O_2S$ nanoparticles

Bimetallic oxysulfides were prepared *via* a solvothermal reaction including a mixture of organic solvents and metallic complexes. Oleylamine (OM; technical grade, 70 %), oleic acid (OA; technical grade, 90 %), sulfur (S_8; ≥ 99.5 %) and sodium oleate (Na(oleate); ≥ 99 %) were purchased from Sigma-Aldrich. 1-Octadecene (ODE; technical grade, 90 %) was purchased from Acros Organics. Gadolinium acetylacetonate hydrate ($Gd(acac)_3 \cdot xH_2O$; 99.9 %) and cerium acetylacetonate hydrate ($Ce(acac)_3 \cdot xH_2O$; 99.9 %) were purchased from Strem Chemicals. All products were used as received without further purification.

In a typical synthesis of $GdCeO_2S$, $Gd(acac)_3 \cdot xH_2O$ (0.25 mmol), $Ce(acac)_3 \cdot xH_2O$ (0.25 mmol), S_8 (0.032 mmol), Na(oleate) (0.50 mmol), OM (17 mmol), OA (2.5 mmol) and ODE (32.5 mmol) were placed in a 100 mL three-neck flask at room temperature. The brown solution was heated to 120 °C under vacuum for 20 min to remove water and other impurities with low boiling points. The mixture was then heated to 310 °C and stirred at this temperature for 30 min under purified N_2. The transparent solution gradually became turbid starting from 280 °C. Then the mixture was left to cool to room temperature under purified N_2. The nanoparticles were isolated using ethanol and washed at least three times using a THF/ethanol (1/5) mixture to remove the remaining reagents and organic matter. A 40 to 90 mg amount of dried $Gd_{2(1-y)}Ce_{2y}O_2S$ particles was thus obtained depending on the initial cerium loading.

It should be noted that a significant decrease in the reaction yield (measured after several washings of the nanoparticles in air) is observed along with the amount of cerium introduced in the nanoparticles: starting from 0.5 mmol of lanthanide precursor, a yield of around 100 % *vs.* Gd (95 mg of powder) was obtained for y = 0 % (Gd_2O_2S) while a yield of 48 % (45 mg) was obtained for y = 70 % ($Gd_{0.6}Ce_{1.4}O_2S$).

Vibrating Sample Magnetometry (VSM)

The magnetization of the nanoparticles was measured between 5 K and 350 K by vibrating sample magnetometry using a Physical Property Measurement System (PPMS) from Quantum Design at the *Physical Measurements at Low Temperature* platform (MPBT) of *Sorbonne Université*. The powder sample (around 10 mg) was placed in a nonmagnetic sample holder and mounted in the magnetometer. A linear motor makes the sample vibrate at 40 Hz thus generating an oscillating magnetic dipole. Zero-field cooling (ZFC) and field cooling (FC) curves were obtained at 50 Oe for most of the samples (2500 Oe for $Gd_{0.2}Ce_{1.8}O_2S$ nanoparticles).

Scanning electron microscopy (SEM) and energy dispersive X-ray spectroscopy (EDS)

A small amount of powder was deposited on a carbon adhesive tape on a scanning electron microscope sample holder. A layer of carbon was deposited on the samples for electronic conductivity. EDS analyses were performed on a SEM HITACHI S-3400N at 10 kV. Titanium was chosen as reference and analyses were performed on three to five different zones on each sample.

X-ray Powder Diffraction (XRD)

The different X-ray diffraction patterns of dry powders were measured on a Bruker D8 diffractometer using Cu Kα radiation at 1.5406 Å. Typical diffractograms were collected with steps of 0.05 ° and a scanning speed of 5 s/point. The backgrounds of the patterns were subtracted using the EVA software. When low noise Si monocristals sample holders were used, the angular position 2θ was corrected by adjusting the sample height (correction around 0.5 to 1 mm).

Acknowledgements

This work was supported by French state funds managed by the ANR within the Investissements d'Avenir programme under reference ANR-11-IDEX-0004-02, and more specifically within the framework of the Cluster of Excellence MATISSE led by Sorbonne Université. Sorbonne Université, CNRS, and the Collège de France are acknowledged for financial support.

References

1 É. Tóth, L. Helm and A. E. Merbach, *Relaxivity of MRI Contrast Agents*, Springer Berlin Heidelberg, Berlin, Heidelberg, 2002, vol. 221.

2 J. W. M. Bulte and D. L. Kraitchman, *NMR Biomed.*, 2004, **17**, 484–499.

3 M. Engström, A. Klasson, H. Pedersen, C. Vahlberg, P.-O. Käll and K. Uvdal, *Magn. Reson. Mater. Physics, Biol. Med.*, 2006, **19**, 180–186.

4 R. M. Petoral, F. Söderlind, A. Klasson, A. Suska, M. A. Fortin, N. Abrikossova, L. Selegård, P.-O. Käll, M. Engström and K. Uvdal, *J. Phys. Chem. C*, 2009, **113**, 6913–6920.

5 D. Kryza, J. Taleb, M. Janier, L. Marmuse, I. Miladi, P. Bonazza, C. Louis, P. Perriat, S. Roux, O. Tillement and C. Billotey, *Bioconjug. Chem.*, 2011, **22**, 1145–1152.

6 S. R. Cherry, *Annu. Rev. Biomed. Eng.*, 2006, **8**, 35–62.

7 Y. Li, Y. Huang, T. Bai and L. Li, *Inorg. Chem.*, 2000, **39**, 3418–3420.

8 J. Dhanaraj, R. Jagannathan and D. C. Trivedi, *J. Mater. Chem.*, 2003, **13**, 1778–1782.

9 F. Zhao, M. Yuan, W. Zhang and S. Gao, *J. Am. Chem. Soc.*, 2006, **128**, 11758–11759.

10 Y.-Z. Huang, L. Chen and L.-M. Wu, *Cryst. Growth Des.*, 2008, **8**, 739–743.

11 Y. Ding, J. Gu, J. Ke, Y.-W. Zhang and C.-H. Yan, *Angew. Chemie Int. Ed.*, 2011, **50**, 12330–12334.

12 J. Gu, Y. Ding, J. Ke, Y. Zhang and C. Yan, *Acta Chim. Sin.*, 2013, **71**, 360.

13 G. Wang, H. Zou, B. Zhang, Y. Sun, Q. Huo, X. Xu and B. Zhou, *Opt. Mater. (Amst).*, 2015, **45**, 131–135.

14 C. Larquet, A.-M. Nguyen, M. Ávila-Gutiérrez, L. Tinat, B. Lassalle-Kaiser, J.-J. Gallet, F. Bournel, A. Gauzzi, C. Sanchez and S. Carenco, *Inorg. Chem.*, 2017, **56**, 14227–14236.

15 W. He, M. E. Osmulski, J. Lin, D. S. Koktysh, J. R. McBride, J.-H. Park and J. H. Dickerson, *J. Mater. Chem.*, 2012, **22**, 16728.

16 R. Ballestracci, E. F. Bertaut and G. Quezel, *J. Phys. Chem. Solids*, 1968, **29**, 1001–1014.

17 G. Quezel, R. Ballestracci and J. Rossat-Mignod, *J. Phys. Chem. Solids*, 1970, **31**, 669–684.

18 V. Biondo, P. W. C. Sarvezuk, F. F. Ivashita, K. L. Silva, A. Paesano and O. Isnard, *Mater. Res. Bull.*, 2014, **54**, 41–47.

19 A. P. Ramirez, *Annu. Rev. Mater. Sci.*, 1994, **24**, 453–480.

Table of Content Image

Luminescent $(Gd,Ce)_2O_2S$ oxysulfide nanoparticles show tunable magnetic properties as a function of their cerium content.